Arch. Metall. Mater. **64** (2019), 3, 953-957

DOI: 10.24425/amm.2019.129479

SANG-HUN LEE*,**, KI-HWAN KIM**#, SEOUNG-WOO KUK**,
JEONG-YONG PARK**, JI-HOON CHOI*

MICROSTRUCTURAL CHARACTERIZATION OF U-10WT.%ZR FUEL SLUGS CONTAINING RARE-EARTH ELEMENTS PREPARED BY MODIFIED INJECTION CASTING

U-10wt.%Zr metallic fuel slugs containing rare-earth (RE: a rare-earth alloy comprising 53% Nd, 25% Ce, 16% Pr and 6% La) elements for a sodium-cooled fast reactor were fabricated by modified injection casting as an alternative method. The distribution, size and composition of the RE inclusions in the metallic fuel slugs were investigated according to the content of the RE inclusions. There were no observed casting defects, such as shrunk pipes, micro-shrinkage or hot tears formed during solidification, in the metallic fuel slugs fabricated by modified injection casting. Scanning electron micrographs and energy-dispersive X-ray spectroscopy (SEM-EDS) showed that the Zr and RE inclusions were uniformly distributed in the matrix and the composition of the RE inclusions was similar to that of a charged RE element. The content and the size of the RE inclusions increased slightly according to the charge content of the RE elements. RE inclusions in U-Zr alloys will have a positive effect on fuel performance due to their micro-size and high degree of distribution.

Keywords: U-Zr, Rare-earth element, Microstructure, Injection casting, Sodium-cooled Fast Reactor (SFR)

1. Introduction

Metallic fuel is a candidate nuclear fuel for a sodium-cooled fast reactor (SFR). Metallic fuel has many advantages: simple fabrication procedures, good neutron economy, high thermal conductivity, excellent compatibility with the sodium coolant, and inherent passive safety [1-3]. Pyro-processing can maximize the utilization of uranium resources from spent fuel and maintain a higher resistance to proliferation. The RE elements from the spent fuel are not separated after pyro-processing because the chemical properties of RE elements are very similar to those of minor actinides in the trans-uranium [4,5]. The preparation of metallic fuel has been produced using various methods such as rolling, swaging, wire drawing, and co-extrusion, but each of these methods is not suitable for remote use due to process limitations that require additional processing and complex preparation equipment [2]. The injection casting is one of the processes that fulfills these needs and it has strong advantages in terms of fabricating small diameter castings with a high L/D ratio and a randomly oriented grain structure, enabling precision castings [2,5]. The U-Zr metallic fuel slugs containing rare-earth elements for a SFR were fabricated using a modified injection casting method [6-8]. Unlike the conventional injection casting that operates under the atmospheric pressure, the modified injection casting method prevents the evaporation of volatile elements in pressurized Ar atmosphere, during melting of metallic fuel [6].

In previous work, the metallic fuel slugs with various RE contents were fabricated, in order to investigate the RE deficiencies in the fuel slugs, the distribution of component in the fuel slugs and melt-residue was discussed [5-8]. In this study, the metallic U-10wt.%Zr fuel slugs containing various levels of RE content (0, 3, 5, and 7 wt.%) were fabricated by a modified injection casting method. RE elements tend to be immiscible with U-Zr alloys and have a significant effect on fuel performance depending on their size and distribution. The distribution of RE elements inclusions in the fuel slug are important in the fuel burning reactors. Because the RE elements react with the cladding material during irradiation, which lowers the eutectic threshold temperature and increasing the thickness of reaction layer [19]. In addition, the uniform distribution of inclusions showed relatively high burnup in the modeling results of uniform and non-uniform distribution [20]. In particular, when a RE element is distributed in the outer area of the metallic fuel slug, it easily reacts with the cladding material to deteriorate the fuel performance [9-12]. This study mainly focused on assessing the microstructure characteristics of RE inclusions, such as uniformity, distribution, composition, content, and phase behaviors in the metallic fuel slugs.

* CHUNGNAM NATIONAL UNIVERSITY, MATERIALS SCIENCE & ENGINEERING DEPARTMENT, DAEJEON, 34134, REPUBLIC OF KOREA
** KOREA ATOMIC ENERGY RESEARCH INSTITUTE, SFR FUEL DEVELOPMENT DIVISION, DAEJEON, 34507, REPUBLIC OF KOREA

Corresponding author: khkim2@kaeri.re.kr

2. Experimental

The U-10 wt.% Zr fuel slugs with various levels of RE content (0, 3, 5, and 7 wt.%) were fabricated by modified injection casting and the RE alloy consisted of 53% Nd, 25% Ce, 16% Pr, and 6% La based on the weight ratio [7,8]. The graphite crucible was coated with yttrium oxide by applying a plasma-spray coating to prevent interaction behavior between the molten uranium alloy and the graphite crucible [13-15]. Quartz tube molds were also slurry-coated with yttrium oxide on the inner surface.

Fig. 1 shows a schematic diagram of the metallic fuel slug fabrication process by injection casting. The starting materials were loaded into a graphite crucible and the initial atmosphere in the chamber was initiated at a vacuum of 1.5×10^{-2} torr up to 500°C (Fig. 1(a)). Then, the pressure of the melting chamber was maintained in an Ar atmosphere of about 400 torr during the heating to prevent the volatilization of the molten material. The U-Zr and U-Zr-RE alloys heated to a temperature of 1550°C and 1470°C, respectively, before the injection casting into the quartz molds (Fig. 1(b)). To prevent volatilization of the molten RE elements, the casting was performed at different casting temperatures. The quartz tube molds were immersed in the molten alloys, and Ar gas was pressurized to cast the metallic fuel slugs into the molds (Fig. 1(c)). The mold was raised after it was held for a few seconds to cool the mold (Fig. 1(d)). The diameter of the cast metallic fuel slugs was 5 mm, with a length of 250 mm (Fig. 1(e)).

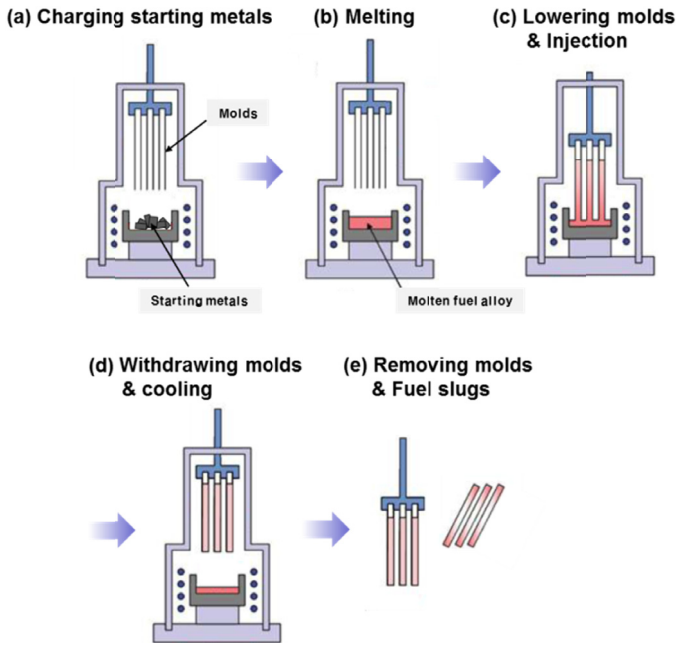

Fig. 1. Schematic diagram of the metallic fuel slugs fabrication process by the modified injection casting method

The density of the metallic fuel slug was measured using Archimedean immersion at the top, middle, and bottom positions of the metallic fuel slug. The microstructures and compositions of the cross-sections of the metallic fuel slugs were examined using a scanning electron microscope (SEM) and a system equipped with an energy-dispersive X-ray spectroscopy (EDS) detector. An image analysis method (iSolution DT image analyzer) was used to measure the area fraction of the inclusions from the cross-sections of the metallic fuel slugs.

3. Results and discussion

The density of the fuel slugs provides indirect information on the existence of internal defects and the alloy content of charge materials. In the injection casting process, injection pressure, casting parameters such as casting temperature, preheating temperature, and mold-coating conditions are closely related to casting defects, and these parameters affect the maintenance of the equal density of the metallic fuel slug at the position. The density variations in the metallic fuel slugs according to RE content are shown in Fig. 2. The average densities of the U-10wt.%Zr, U-10wt.%Zr-3wt.%RE, U-10wt.%Zr-5wt.%RE and U-10wt.%Zr-7wt.%RE metallic fuel slugs were measured as approximately 15.5 $g \cdot cm^{-3}$, 15.1 $g \cdot cm^{-3}$, 14.9 $g \cdot cm^{-3}$ and 14.8 $g \cdot cm^{-3}$, respectively. Immiscible RE elements were not entirely incorporated in the U-Zr molten metal, but floated during melting. The top layer of the molten metal affected the RE contents of the slugs, because the injection mold assembly was placed in the middle of the molten metal [8]. Especially, the density of U-10Zr-7RE fuel slug was lower at the bottom, because it contained relatively large amount of RE elements floated on the top of the molten metal. Although the densities of the metallic fuel slugs had a little variation based on the position, these densities were close to the average density of the fuel slugs. Compared with the theoretical density, the measured density of the U-10Zr fuel slug had a somewhat low density, which might have originated from impurities and micro-pores in the metallic fuel slug. The measured density was similar to the theoretical density in the U-Zr-RE fuel slug as the RE content increases. The result that the densities measured for the U-Zr containing RE fuel slugs are higher than predicted is assumed to be because

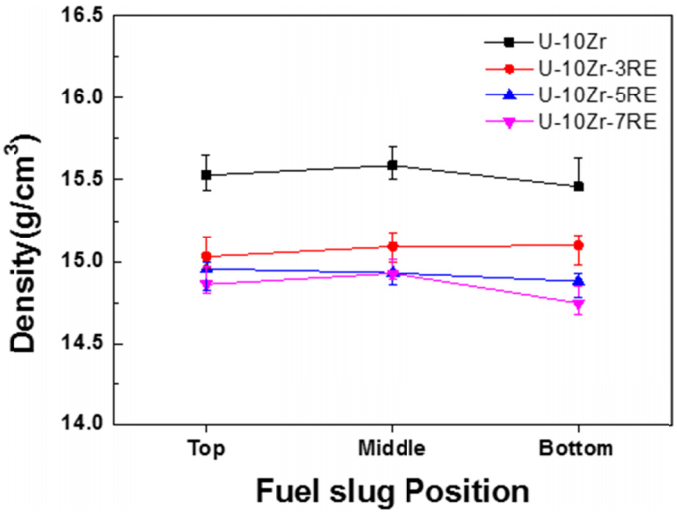

Fig. 2. The density variations in the metallic fuel slugs according to RE element content

the reactive RE elements were not retained within the slug during the casting process. The RE oxide will form preferentially than the U and Zr oxides during the casting process. Thus, the RE elements can be incorporated in the casting dross rather than the fuel slug. This will relatively increase the content of element U in the fuel slug [8].

Fig. 3 shows back-scattered electron micrographs of the cross-section of metallic fuel slugs according to RE content. Fig. 4 shows high magnification images of Fig. 3, with EDS results listed in Tables 1 to 4. The inclusions are similarly distributed from the center of the metallic fuel slug to the outer area. As shown in Fig. 3(a) and Fig. 4(a), the inclusions with globular and needle-like shapes were observed in the matrix. The inclusions were uniformly distributed in sizes smaller than 10 μm, and some of the inclusions were observed adjacent to each other. The composition analyses showed that the inclusions were the Zr-rich phase containing a small amount of U, C and O elements (Table 1). The Zr-rich phase in the U-10Zr alloy is not formed according to the phase diagram of the U-Zr alloy [16]. It has been inferred that trace impurities such as C, N, and O from the charge materials are involved in formation of the inclusions [8,17,18].

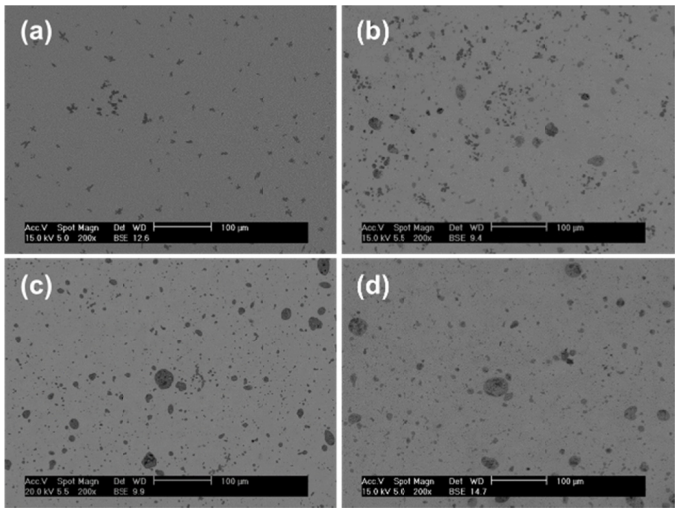

Fig. 3. Cross-sectional back-scattered scanning electron micrographs of metallic fuel slugs: (a) U-10wt.%Zr, (b) U-10wt.%Zr-3wt.%RE, (c) U-10wt.%Zr-5wt.%RE, (d) U-10wt.%Zr-7wt.%RE

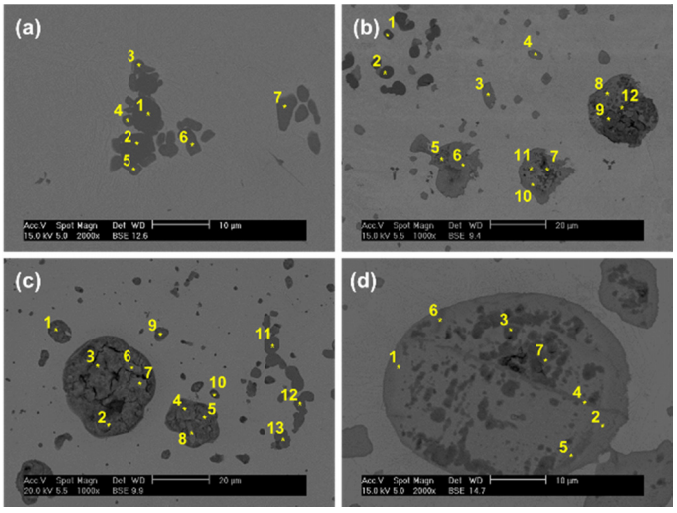

Fig. 4. A higher magnification region from the images shown in Fig. 3. The composition analysis points are marked with numbers

TABLE 1

Composition analysis of the U-10wt.%Zr fuel slug measured using EDS in Fig. 4(a). Values in weight %

Location	U	Zr	C	O
Matrix	91.6	6.7	1.7	□
#1	□	84.3	13.2	2.5
#2	□	84.8	13.4	1.8
#3	3.4	93.8	□	2.8
#4	2.4	94.4	□	3.2
#5	2.0	94.7	□	3.3
#6	2.2	94.2	□	3.6
#7	1.8	94.7	□	3.5

Two different inclusions were randomly dispersed in the U-Zr matrix and there was no agglomeration of the inclusions in any of the metallic fuel slugs, as shown in Figs. 3(b), (c) and (d). The Zr-rich phase with a shape similar to the one shown in Fig. 3(a) was also observed in Figs. 3(b), (c) and (d). Not only U, C, and O elements but also the Hf element estimated as impurities contained in the Zr raw material were detected in this Zr-rich phase (Tables 1 and 2). The charged RE elements did not react with the molten U-Zr alloy due to their immiscibility. Spherical RE inclusions of less than 40 μm were located in the matrix, and the size of the RE inclusions increased slightly with an increasing charged RE content. The composition analysis revealed that the RE inclusions were similar to the charge content of the RE element in points 3-9 in Fig. 4(b) and Table 2, points 1-5 in Fig. 4(c) and Table 3, and points 1-3 in Fig. 5(d) and Table 4. The RE phases containing Y in the RE inclusions were analyzed as observed in points 10 and 11 in Fig. 4(b) and Table 2, points 6-8 in Fig. 4(c) and Table 3, and points 4 and 5 in Fig. 4(d) and Table 4. As given in Table 4, the EDS analysis results show RE inclusions containing Zr_2Si (point 6) and a Zr-

TABLE 2

Composition analysis of the U-10wt.%Zr-3wt.%RE fuel slug measured using EDS in Fig. 4(b). Values in weight %

Location	U	Zr	Nd	Ce	Pr	La	Y	Hf	C	O
Matrix	91.0	7.6	□	□	□	□	□	□	□	1.4
#1	□	96.6	□	□	□	□	□	1.5	□	1.9
#2	□	86.8	□	□	□	□	□	4.0	7.4	1.8
#3	□	□	50.4	26.4	16.8	3.2	□	□	1.7	1.5
#4	□	□	46.4	29.0	15.1	4.5	□	□	2.3	2.7
#5	□	□	49.8	17.2	15.0	9.3	□	□	3.2	5.5
#6	□	□	50.2	18.3	15.1	10.2	□	□	2.8	3.4
#7	□	□	45.1	17.5	14.9	8.1	□	□	3.3	11.1
#8	□	□	48.7	18.2	15.5	10.0	□	□	2.8	4.8
#9	□	□	41.1	15.2	14.0	8.4	□	□	3.39	17.9
#10	2.8	□	37.9	11.6	11.2	5.4	18.0	□	2.9	10.2
#11	□	□	37.4	7.5	8.7	3.0	29.2	□	3.6	10.6

TABLE 3

Composition analysis of the U-10wt.%Zr-5wt.%RE fuel slug measured using EDS in Fig. 4(c). Values in weight %

Location	U	Zr	Nd	Ce	Pr	La	Y	Hf	C	O
Matrix	90.4	7.8	□	□	□	□	□	□	□	1.8
#1	□	□	44.0	27.8	12.6	2.0	□	□	4.7	8.9
#2	□	□	43.9	15.7	12.9	4.0	□	□	5.6	17.9
#3	□	□	47.2	17.0	12.8	4.5	□	□	8.3	10.2
#4	□	□	42.7	15.7	12.3	4.0	□	□	6.9	18.4
#5	□	□	44.2	19.2	13.6	4.6	□	□	7.1	11.3
#6	□	□	48.4	7.9	9.8	2.8	15.7	□	4.2	11.2
#7	□	□	48.1	9.2	9.4	3.6	15.3	□	3.6	10.8
#8	□	□	37.9	7.1	7.9	1.6	20.5	□	8.8	16.2
#9	4.0	□	39.0	25.0	12.4	1.9	□	□	8.3	9.4
#10	11.0	□	37.3	21.0	12.6	0.2	□	□	8.0	9.9
#11	□	84.5	□	□	□	□	□	4.8	9.3	1.4
#12	□	84.6	□	□	□	□	□	5.0	8.8	1.6
#13	□	84.2	□	□	□	□	□	5.1	9.2	1.5

TABLE 4

Composition analysis of the U-10wt.%Zr-7wt.%RE fuel slug measured using EDS in Fig. 4(d). Values in weight %

Location	U	Zr	Nd	Ce	Pr	La	Y	Si	C	O
Matrix	90.4	9.6	□	□	□	□	□	□	□	□
#1	□	□	53.2	22.9	16.3	4.6	□	□	3.0	□
#2	□	□	52.4	23.6	16.6	4.5	□	□	2.9	□
#3	□	□	53.4	23.1	15.9	4.5	□	□	3.0	0.1
#4	□	□	48.2	12.0	11.1	2.3	16.2	□	5.6	4.6
#5	□	□	51.5	23.3	16.3	5.1	0.3	□	3.5	□
#6	□	19.6	43.6	17.9	12.7	2.8	□	3.2	□	0.2
#7	□	74.8	4.4	1.8	1.3	0.1	□	□	14.5	3.1

rich phase (point 7). Si and Y elements were included in the reaction with the RE elements by the quartz tube mold and the protective coating layer, respectively. Regardless of the increase in RE content in the metallic fuel slugs, the compositions of the RE inclusions were measured similar to the composition of the charged RE alloy. It is likely that the Y element is mainly detected in the RE inclusion because it can easily penetrate into the Y_2O_3 coating layer due to the chemical reactivity of the RE elements. As shown EDS points 3-7 in Fig. 3(a) and Table 1, and point 10 in Fig. 3(b) and Table 2, and points 9 and 10 in Fig. 3(c) and Table 3, due to the small size of the RE inclusions or the Zr-rich phase, the amount of the surrounding U in the matrix was detected during the EDS analyses.

Fig. 5 shows the area fraction occupied by the inclusions from the center to the outer area for cross sections of the metallic fuel slugs. It is considered that the amount of the inclusions for the U-10wt.%Zr fuel slug is the area fraction of Zr inclusions, and that the amount of the inclusions for the U-Zr-RE fuel slugs is the area fraction of Zr and RE inclusions, as shown in Fig. 4 and Tables 1-4. The area fraction of the inclusions was the highest at the outer area in the U-10wt.%Zr and U-10wt.%Zr-7wt.%RE fuel slugs, and the highest at the center area in the U-10wt.%Zr-3wt.%RE and U-10wt.%Zr-5wt.%RE fuel slugs. In other words, it can be seen that the inclusions are uniformly distributed in the respective metallic fuel slugs from the center to the outer area without any bias in a specific area. When the RE elements are in specific locations, especially where there is a large amount in the outer area of the fuel slug, which results in a reaction with the stainless cladding during the irradiation and the reaction products to form phases with a low melting temperature.

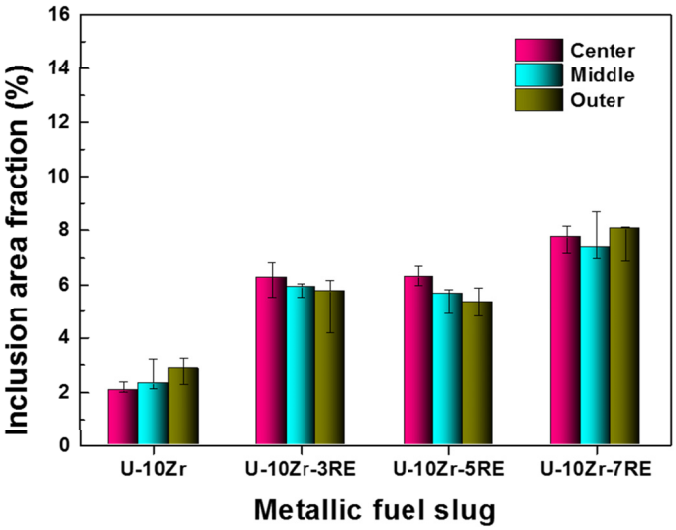

Fig. 5. Variation in the area fraction of inclusions from the center area to the outer area according to RE element content

The area fraction of the inclusions in the metallic fuel slug containing RE elements increased slightly as the RE content increase because they increase the size of the inclusions as well as the content of the inclusions, as mentioned above (Fig. 3 and Fig. 4). However, these results confirmed that the area fraction of the RE inclusions was somewhat low with respect to the nominal content of the RE elements. We assumed that the area fraction of the inclusions in the U-10wt.%Zr-5wt.%RE fuel slug was slightly lower than that in the U-10wt.%Zr-3wt.%RE fuel slug because of an error by the area measurement and by the amount of charge materials during injection casting.

4. Conclusions

The U-10wt.%Zr metallic fuel slugs containing 0, 3, 5, 7wt.% RE elements were soundly fabricated to the full length of the mold without significant cracks using a modified injection casting. The measured density of the U-Zr fuel slug was lower than the theoretical density and the measured density of the U-Zr-RE fuel slug was higher than the theoretical density due to the low content of the RE element with a low density. Zr and RE inclusions were uniformly distributed in the matrix from the center to the outer areas in a cross section of the metallic fuel slug. The composition of the RE inclusions was similar to that of a charged RE, and the RE inclusions were present in sizes of less than 40 μm. The RE content and the size of the RE inclusions increased slightly depending on the charge content of RE

elements. Therefore, the modified injection casting method is a promising candidate fabrication method for metallic fuel slugs containing RE element content.

Acknowledgments

This work has been carried out under the Nuclear Research and Development Program supported by the Ministry of Science and Technology in the Republic of Korea.

REFERENCES

[1] L.C. Walters, J. Nucl. Mater. **207**, 39-48 (1999).
[2] D.E. Burkes, R.S. Fielding, D.L. Porter, D.C. Crawford, M.K. Meyer, J. Nucl. Mater. **389**, 458-469 (2009).
[3] D.C Crawford, D.L. Porter, S.L. Hayes, J. Nucl. Mater. **371**, 202-231 (2007).
[4] M. Sakata, M. Kurata, T. Hijikata, T. Inoue, J. Nucl. Mater. **185**, 56-65 (1991).
[5] J. H. Kim, H. Song, K.H. Kim, C.B. Lee, J. Radioanal. Nucl. Chem. **301**, 797-803 (2014).
[6] J. H. Kim, K.H. Kim, C.B. Lee, Adv. Mater. Sci. Eng. **2015** (2015).
[7] J. H. Kim, J.W. Lee, K.H. Kim, J.Y. Park, J. Nucl. Sci. Technol. **54**, 648-654 (2017).
[8] S.W. Kuk, K.H. Kim, J.H. Kim, H. Song, S.J. Oh, J.Y. Park, C.B. Lee, Y.S. Youn, J.Y. Kim, J. Nucl. Mater. **486**, 53-59 (2017).
[9] D.D Keriser Jr., M.C. Pertri, J. Nucl. Mater. **240**, 51-61 (1996).
[10] T. Ogata, M. Kurata, K. Nakamura, A. Itoh, M. Akahori, J. Nucl. Mater. **250**, 171-175 (1997).
[11] K. Nakamura, T. Ogata, M. Kurata, A Itoh, M. Akahori, J. Nucl. Mater. **275**, 246-254 (1999).
[12] H.J. Ryu, B.O. Lee, S.J. Oh, J.H. Kim, C.B. Lee, J. Nucl. Mater. **392**, 206-212 (2009).
[13] J.E. Indacochea, S. Mcdeavitt, G.W. Billings, Adv. Eng. Mater. **3**, 895-901 (2001).
[14] K.H. Kim, C.T. Lee, C.B. Lee, R.S Fielding, J.R Kennedy, J. Nucl. Mater. **441**. 535-538 (2013).
[15] J.H. Kim, H. Song, K.H. Kim, C.B. Lee, Surf. Interface Anal. **47**, 301-307 (2015).
[16] F.A Rough, Report No. BMI-1030, Battelle Memorial Institute, Metallurgy and ceramics, M-3697, 16th Ed. (1955).
[17] D.E. Janney, J. R. Kennedy. Mater. Charact. **61**, 1194-1202 (2010).
[18] D.E. Janney, T.P. O'Holleran. J. Nucl. Mater. **460**, 13-15 (2015).
[19] K. Inagaki, T. Ogata. J. Nucl. Mater. **441**, 574-757 (2013).
[20] Al. Qaaod, H. Shahbunder, R.M. Refeat, E.A. Amin, S.U. El-Kamessy, Annals of Nuclear Energy. **121**, 101-107 (2018).